Theoretical Study of Platinum Doped Anatase (101) Surface on Detecting Decomposition Production of Polyvinyl Chloride

Ling NIE [1], Changli ZHOU [1], Yi AO [1], Zhengqin CAO [1] *, Gang WEI [1], Qiming LUO [1], Ke WU [2], Gang Hu [1]

[1] *College of Electrical Engineering, Chongqing University of Science and Technology, Chongqing 401331, China*
[2] *State Grid Chongqing Electric Power Company, Chongqing 400014, China*

http://doi.org/10.5755/j02.ms.32435

Received 6 October 2022; accepted 31 March 2023

The gas sensitivity of platinum doped TiO_2 (101) to two kinds on polyvinyl chloride decomposition production, CO and HCl, were explored based on density functional theory. The binding energy, adsorption distance, charge transfer, and density of states distribution were simulated and discussed. The results suggest that the O oriented mode is probably the best mode for the CO gas molecules adsorption on the Pt-TiO_2 and H oriented mode for the HCl adsorption system. HCl and CO molecules obtain electrons from Pt doped TiO_2 surface. At room temperature, the recovery time of CO and HCl is 1.9743×10^{-10}, 1.2094×10^{-10} respectively. HCl is easier to dissociate from Pt doped TiO_2 surface with a little lower energy barrier compared to CO. This work provides theoretical adsorption information of Pt-TiO_2 as gas sensor material for HCl and CO detection in the application of online condition monitoring and defect diagnosis in the power cables.
Keywords: polyvinyl chloride, Pt doping, TiO_2, gas sensitivity, CO, HCl.

1. INTRODUCTION

Polyvinyl chloride (PVC) has been widely utilized in the outer sheath of power cable, due to the advantage of good abrasion resistance and insulation characteristics, etc [1 – 3]. However, the thermal stability of PVC is poor leading to it being easy to decompose and generate CO, HCl and other gases under overheating defects [4 – 7]. Moreover, the formation characteristics of these decomposition products are significantly related to the thermal decompose temperature [8]. As a result, the early fire warning of power cable could be realized effectively via the detection of the decomposition gases of PVC based on gas sensors [9].

As such material with remarkably high gas sensitivity properties and stability [10 – 12], anatase TiO_2 (101) has been getting wide attention. In addition, the gas sensitivity property of materials could be improved significantly via noble metal doping on the surface [13, 14]. For TiO_2, Gui et al found that Pt doped TiO_2 performs a nice gas-sensitivity performance on SOF_2, SO_2F_2, and SO_2 [15 – 17]. Zhang studied the gas sensitivity and sensing mechanism of Au-doped TiO_2 for SF_6 decomposition components [18].

In this paper, two gas sensitivity properties of characteristic decomposition products of PVC, namely CO and HCl, on Pt-doped anatase TiO_2 (101) (Pt-TiO_2) were investigated based on the density functional theory (DFT). The binding energy, charge transfer, density of states, the distributions of occupied molecule orbital were analysed. All results provide theoretical information for the application of Pt-TiO_2 in the online monitor of fire fault of power cable.

* Corresponding author. Tel.: 15922798290; fax: 023 6502 2368.
E-mail: *caozhengqin@vip.sina.com* (Z. Cao)

2. METHODS

The spin-polarized calculations were implemented by $Dmol^3$ package in this paper [19]. All the structures were optimized via general gradient approximate (GGA) with Perdew-Burke-Ernzerho (PBE) function [20]. The global orbital cutoff radius was selected as 5.0 Å to ensure the accurate calculation results of total energy [21, 22]. The K-points of the Brillouin zone are sampled as 2 × 3 × 1 by the Monkhorst-Packscheme method. Tkatchenko and Scheffler’s (TS) DFT-D method was adopted for a better consideration of the dispersion forces [23]. The convergence threshold, energy tolerance accuracy, and maximum atom displacement were selected as 0.002 Ha/Å, 1.0×10^{-5} Ha, and 5×10^{-3} Å, respectively [24].

The binding energy $E_{binding}$ of CO, HCl gas molecules adsorbed on Pt-TiO_2 surface is determined as the Eq. 1 [25 – 28]:

$$E_{binding} = E_{gas/Pt-TiO2} - E_{gas} - E_{Pt-TiO2}\,, \tag{1}$$

where $E_{gas/Pt-TiO2}$, E_{gas}, and $E_{Pt-TiO2}$ represent the total system energy after gas molecules adsorption, the energy of isolated gas molecules, and the energy of intrinsic Pt-TiO_2 surface, respectively.

The charge transfer Q_t was obtained via Hirshfeld analysis charge population [29, 30]. If the $Q_t > 0$, it denotes the gas molecules donated electrons to the Pt-TiO_2 surface during the adsorption process. If the $Q_t < 0$, it indicates the electrons transfer from the Pt-TiO_2 surface to gas molecules during the adsorption process.

3. RESULTS AND DISCUSSION

3.1. The Pt-doped anatase TiO_2 (101) surface

Based on the previous research [16], the size of the (101) surface supercell is 10.88 Å × 11.32 A˚ × 24.35 A.

The height of the vacuum above the surface is approximately 16 Å to prevent the interaction between adjacent cells. And one Pt atom dopes between two O atoms of TiO_2 is the most stable structure. Both bond lengths of Pt-O are 2.371 Å, and the bond angle of O-Pt-O is 96.119°. The optimized structures of the Pt-TiO_2 surface are shown in Fig. 1. Fig. 2 shows the density of state (DOS) of the intrinsic anatase TiO_2 (101) surface and the Pt-doped TiO_2 anatase surface. In Fig. 2, we observed that the doped Pt atoms connected the valence band and conduction band separated on the intrinsic TiO_2 surface, improving the surface conductivity effectively.

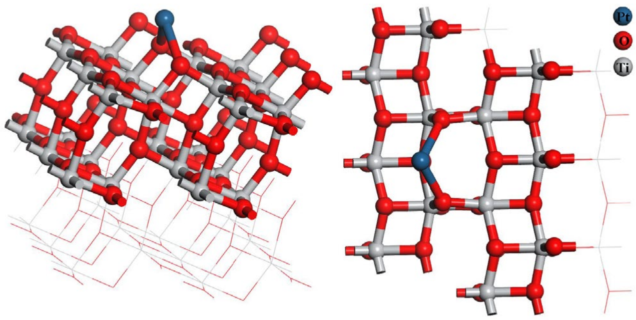

Fig. 1. Views of Pt doped TiO_2 (101) surface

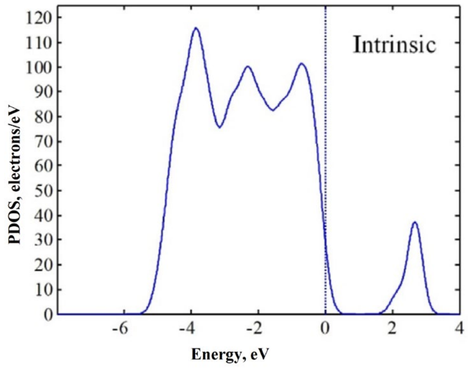

a

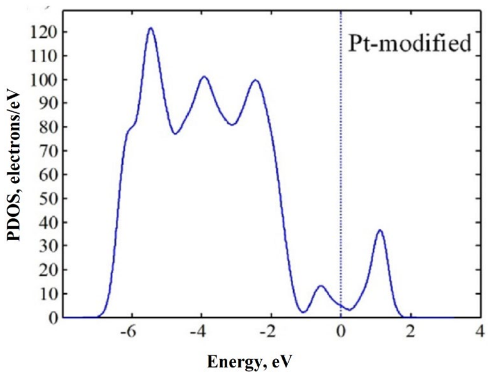

b

Fig. 2. DOS of the TiO_2 (101) surface and Pt-TiO_2 (101) surface: a – TiO_2 (101); b – Pt-TiO_2 (101)

Fig. 3 shows the energy gap between the intrinsic anatase TiO_2 (101) surface and the Pt-doped TiO_2 anatase surface. The energy gap after Pt atom doping is 0.439 eV, which is 1.722 eV less than the intrinsic TiO_2 energy gap of 2.161 eV. The smaller the band gap, the easier it is for electrons to be excited from the valence band to the conduction band, the higher the intrinsic carrier concentration and the higher the conductivity.

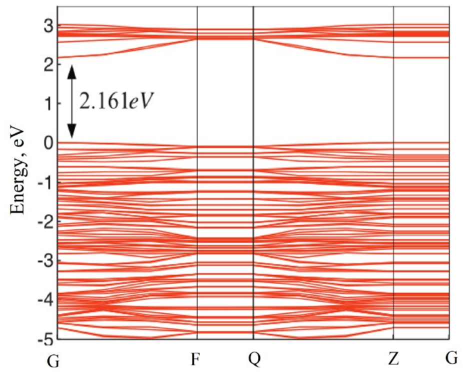

a

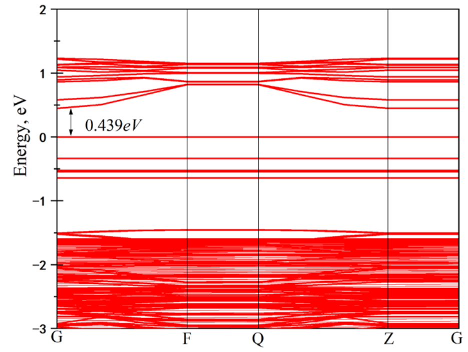

b

Fig. 3. Energy gap of the TiO_2 (101) surface and Pt-TiO_2 (101) surface: a – TiO_2 (101); b – Pt-TiO_2 (101)

3.2. Adsorption property of CO on Pt-TiO_2 surface

The bond length of C-O in the optimized structure of the CO gas molecule is 1.142 Å. When simulating the adsorption process of CO on the Pt-TiO2 surface, two initial adsorption modes are considered. One is the C atom of the CO molecule oriented to the Pt atom of the Pt-TiO_2 surface (C-oriented mode). Another adsorption configuration is the O atom of the CO molecule oriented to the Pt atom of the Pt-TiO_2 surface (O-oriented mode).

The optimized adsorption configurations of CO on the Pt-TiO_2 surface are exhibited in Fig. 4 and the relevant adsorption parameters are shown in Table 1. For C-oriented mode, the adsorption distance is 1.970 Å, and the binding energy is -0.326 eV. In addition, there is just -0.0121 e electrons transfered from CO to the Pt-TiO_2 surface during the adsorption process. As for O-oriented mode, the binding energy of 1.305 eV and the charge transfer of -0.0324 e are quite higher than those under C-oriented mode. At the same time, the adsorption distance is 1.713 Å. All of these indicates that the O oriented mode is probably the best mode for the CO gas molecules' adsorption on the Pt-TiO_2 surface.

Table 1. Parameters of CO adsorbed on the Pt-TiO_2 surface in two kinds of oriented modes

Adsorption configurations	Distance, Å	$E_{binding}$, eV	Q_t, e
C-oriented mode	1.970	-0.326	-0.0121
O-oriented mode	1.713	1.305	-0.0324

Table 2 compares the adsorption parameters between CO and different oxides [29, 30]. The results show that the adsorption distance of CO on SnO_2 (110) and β-MnO_2 (110) is larger than Pt-TiO_2 (101), and the adsorption energy is smaller than Pt-TiO_2 (101). This shows that CO is more suitable for adsorption on Pt-TiO_2 (101).

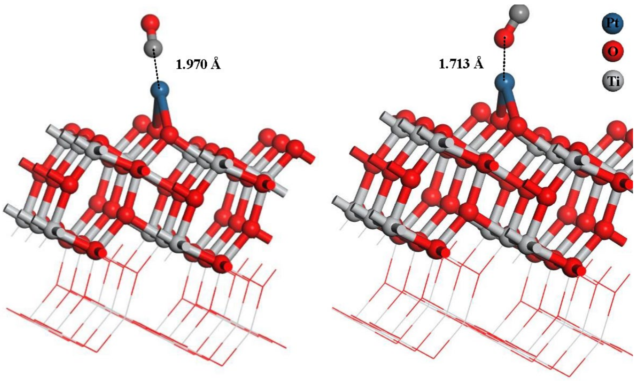

a b

Fig. 4. The optimized adsorption configurations of CO on Pt-TiO_2 surface: a – C-oriented mode; b – O-oriented mode

Table 2. Adsorption parameters of CO on different oxides

Oxide	Distance, Å	$E_{binding}$, eV	Q_t, e
SnO_2 (110)	2.500	-0.560	-0.122
β-MnO_2 (110)	2.064	-0.536	0.110
Pt-TiO_2 (101)	1.713	1.305	-0.0324

The total density of states (TDOS) and partial density of states (PDOS) configuration for CO adsorbing on Pt-TiO_2 surface are analyzed to explore the electronic properties, and they are shown in Fig. 5 and Fig. 6. 0 eV refers to Fermi level.

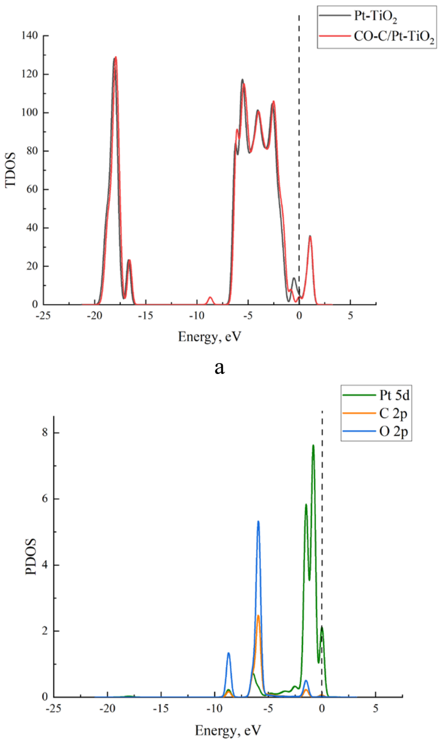

a

b

Fig. 5. Density of states configuration of CO adsorbing on Pt-TiO_2 surface in C oriented mode: a – TDOS; b – PDOS

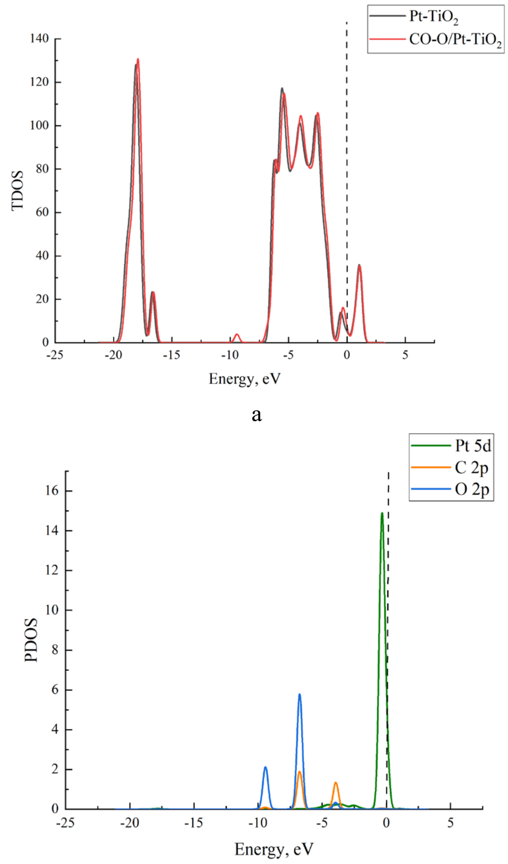

a

b

Fig. 6. Density of states configuration of CO adsorbing on Pt-TiO_2 surface in O oriented mode: a – TDOS; b – PDOS

The DOS in C oriented mode is shown in Fig. 5. The TDOS near the Fermi level decreased obviously and there is a new peak appearing at -8 eV after CO adsorption. According to PDOS, the 2p orbitals of C, O atoms and the 5d orbital of the Pt atom overlapped around -7 eV. The DOS in O oriented mode is shown in Fig. 6. One can find that the TDOS after CO adsorption is similar to that before adsorption. However, TDOS shifted to the right at about 0.3 eV and there also a new peak appeared at -9.5 eV after CO adsorption. According to PDOS results, the 2p orbital of O atoms and 5d orbital of the Pt atom overlapped around -4 eV. In addition, it is worth noting that the peak value 5d orbital of Pt atom in O-oriented mode is quite higher than that in C-oriented mode, which indicates there are more electrons transferred from Pt-TiO_2 to CO in O-oriented mode than in C-oriented mode. And the result is consistent with the Hirshfeld charge population analysis.

3.3. Adsorption property of HCl on Pt-TiO_2 surface

For the adsorption of HCl, two initial adsorption modes are considered as well, namely, the H atom of the HCl molecule oriented to the Pt atom of the Pt-TiO_2 surface (H-oriented mode) and the Cl atom of the HCl molecule oriented to the Pt atom of the Pt-TiO_2 surface (Cl-oriented mode). As for H oriented mode, the binding energy is 1.184 eV with an adsorption distance of 1.910 Å. At the same time, -0.1031 e electrons transfer from the Pt-TiO_2 surface to the HCl molecule during adsorption. In addition, the bond length of H-Cl increased from 1.289 Å to 1.354 Å and the two bond lengths of O-Ti changed to 2.418 and 2.410 Å. For Cl-oriented mode, the adsorption distance of 2.245 Å and charge transfer of -0.1296 e is quite longer than those that in H oriented mode. And the binding energy is 0.359 eV. It is worth noting the deformation of HCl molecules and Pt-TiO_2 surface. The bond length H-Cl of the HCl molecule increases to 2.159 Å. Two bond lengths of O-Ti changed to 2.220 and 3.493 Å and Pt atom is closer to the intrinsic TiO_2 surface after adsorption.

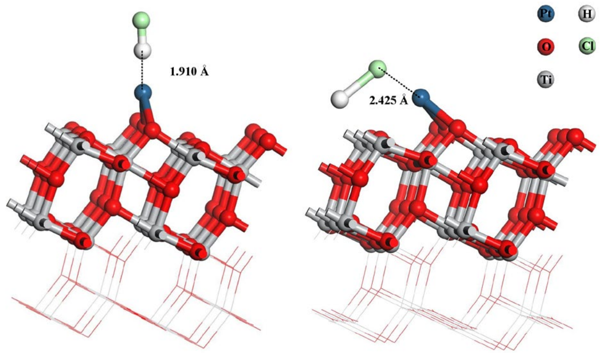

a b

Fig. 7. The optimized adsorption configurations of HCl on Pt-TiO_2 surface: a – H-oriented mode; b – Cl-oriented mode

Table 3. Parameters of HCl adsorbed on the Pt-TiO_2 surface in two kinds of oriented modes

Adsorption configurations	Distance, Å	$E_{binding}$, eV	Q_t, e
H-oriented mode	1.910	1.184	-0.1031
Cl-oriented mode	2.425	0.359	-0.1296

The optimized adsorption configurations of HCl on the Pt-TiO2 surface are exhibited in Fig. 7 and the relevant adsorption parameters are shown in Table 3. The configurations of DOS for HCl adsorbing on Pt-TiO_2 surface are exhibited in Fig. 8 and Fig. 9. For H oriented mode, TDOS shifted to the left about 0.1 eV after HCl adsorption, which indicated that the system becomes more stable and the electrons move towards the low energy position after adsorption. In addition, there is a new small peak that appeared at -14.5 eV. According to the configuration of PDOS, the 5d orbital of Pt overlapped around -1 eV with the 3p orbital of Cl. The 5d orbital of Pt, the 3p orbital of Cl and the 1s orbital of H overlapped with each other around -6 eV, which implies a hybridization between these atomic orbitals and indicates that the interaction between HCl molecule and Pt-TiO_2 surface is strong.

For Cl-oriented mode, there are two new peaks that appeared around -13 and -8 eV after adsorption. Compared with the TDOS configurations of thr Pt-TiO_2 surface, the energy gap after HCl adsorption via Cl-oriented mode decreases from 0.468 eV to 0.448 eV. In addition, the peak value of the 5d orbital of the Pt atom in Cl-oriented mode is larger than that in H-oriented mode, indicating that more charger transfer happened in Cl-oriented mode during the adsorption process and meeting the results of Hirshfeld charge population analysis.

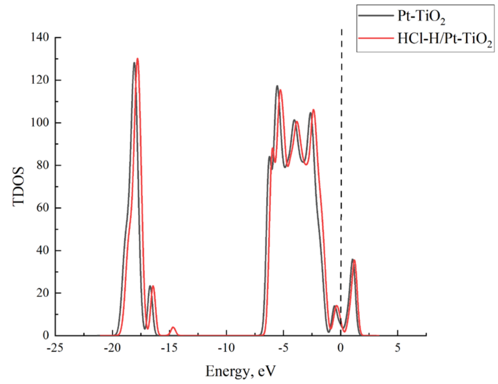

a

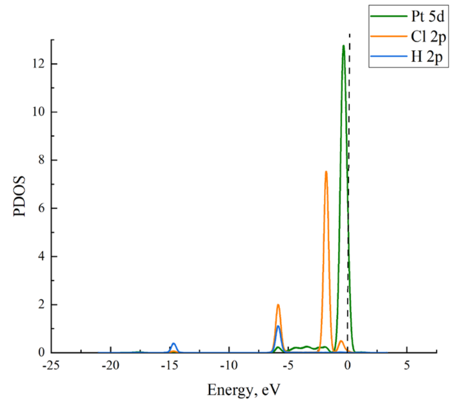

b

Fig. 8. Density of states configuration of HCl adsorbing on Pt-TiO_2 surface in H oriented mode: a – TDOS; b – PDOS

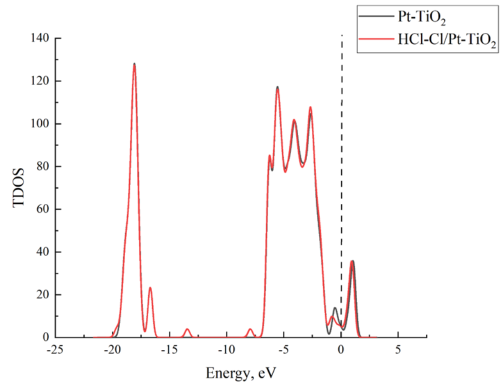

a

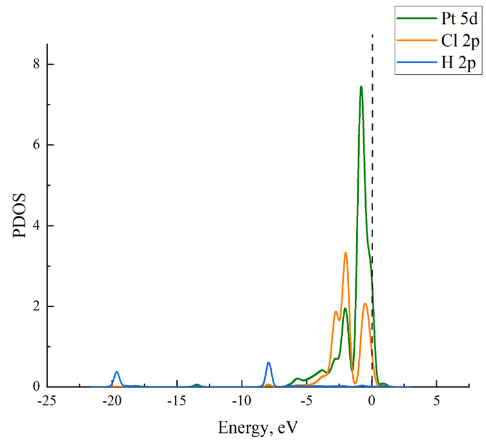

b

Fig. 9. Density of states configuration of CO adsorbing on Pt-TiO_2 surface in O oriented mode: a – TDOS; b – PDOS

3.4. The recovery properties of CO and HCl on Pt-TiO_2 surface

To evaluate the gas sensitivity of CO and HCl on the Pt-TiO_2 surface comprehensively, the recovery properties are also analyzed. The key parameter of recovery properties is the recovery time τ and it can be defined based on the Van't-Hoff-Arrhenius expression and transition state theory [33, 34], as shown in Eq. 2:

$$\tau = A^{-1} e^{(-E_{de}/RT)}, \quad (2)$$

where A represents the apparent frequency factor; E_{de} is the desorption energy; R is the Boltzmann constant; T is the temperature (unit K). It can be considered that the value of the desorption energy is the same as that of binding energy. Assuming A does not change in different gas molecules adsorption [35, 36], the smaller the $E_{binding}$ is, the shorter the τ is under the same temperature. According to the formula, the recovery time of CO at room temperature $\tau = 1.9743 \times 10^{-10}$, the recovery time of HCl at room temperature $\tau = 1.2094 \times 10^{-10}$. Comparing the binding energies, the difficulty of desorption and recovery property of HCl on molecule on Pt-TiO_2 surface could be better than those of CO molecule, the faster the resolution speed is, the better the reversibility of the sensor can be achieved.

4. CONCLUSIONS

In this paper, the gas sensitivity of Pt doped TiO_2 (101) to gas molecules CO and HCl was investigated via adsorption structure, binding energy, adsorption distance, charge transfer, DOS and recovery properties based on DFT. The conclusion can be summarized as followed:

1. The O oriented mode is probably the best mode for the CO gas molecules adsorption on the Pt-TiO_2 and H oriented mode for the HCl adsorption system. The binding energy of the CO adsorption system in O oriented mode is a little bigger than that of the HCl adsorption system in H oriented mode.
2. The recovery time of HCl is better than that of CO, which reversibility is more suitable as the selection gas of the sensor.
3. Pt-TiO_2 surface could be more suitable for the detecting of HCl.

All the works provide theoretical adsorption information of Pt-TiO_2 as gas sensor material for HCl and CO detection in the application of online condition monitoring and defect diagnosis in the power cables.

Acknowledgments

We gratefully appreciate the support of the Science and Technology Research Program of Chongqing Municipal Education Commission (Grant No. KJQN202001524, Grant No. KJZD-K202001505), Chongqing Natural Science Foundation (cstc2020jcyj-msxmX0267), Chongqing Research Program of Technology Innovation and Application Development (No. cstc2020jscx-msxmX0188) and Chongqing Market Supervision Administration Research Program (No. CQSJKJ2020008).

REFERENCES

1. **Shea, J.J.** Identifying causes for Certain Types of Electrically Initiated Fires in Residential Circuits *Fire and Materials* 35 (1) 2011: pp. 19–42. https://doi.org/10.1002/fam.1033
2. **Courty, L., Garo, J.P.** External Heating of Electrical Cables and Auto-ignition Investigation *Journal of Hazardous Materials* 321 2017: pp. 528–536. https://doi.org/10.1016/j.jhazmat.2016.09.042
3. **Passalacqua, R., Cortes, P., Taylor, N., Beltran, D., Zavaleta, P., Charbaut, S.** Experimental Characterisation of ITER Electric Cables in Postulated Fire Scenarios *Fusion Engineering and Design* 88 (9–10) 2013: pp. 2650–2654. https://doi.org/10.1016/j.fusengdes.2013.01.026
4. **Bene, M., Milanov, N., Matuschek, G., Kettrup, A., Balek, V.** Thermal Degradation of PVC Cable Insulation Studied by Simultaneous TG-FTIR and TG-EGA Methods *Journal of Thermal Analysis and Calorimetry* 78 (2) 2004: pp. 621–630. https://doi.org/10.1023/B:JTAN.0000046123.59857.ad
5. **Salovey, R., Bair, H.E.** Degradation of Poly (Vinyl Chloride) *Journal of Applied Polymer Science* 14 (3) 1970: pp. 713–721. https://doi.org/10.1002/app.1970.070140315
6. **Sakata, J.** Thermal Decomposition of Flame-retarded High-Impact Polystyrene *Journal of Analytical and Applied Pyrolysis* 68 (12) 2003: pp. 83–99. https://doi.org/10.1016/S0165-2370(03)00075-5
7. **Zhu, H.M., Jiang, X.G., Yan, J.H., Chi, Y., Cen, K.F.** TG-FTIR Analysis of PVC Thermal Degradation and HCl Removal *Journal of Analytical and Applied Pyrolysis* 82 (1) 2008: pp. 1–9. https://doi.org/10.1016/j.jaap.2007.11.011
8. **Wang, Z., Wei, R., Wang, X., He, J., Wang, J.** Pyrolysis and Combustion of Polyvinyl Chloride (PVC) Sheath for New and Aged Cables via Thermogravimetric Analysis-Fourier Transform Infrared (TG-FTIR) and Calorimeter *Materials* 11 (10) 2018: pp. 1997. https://doi.org/10.3390/ma11101997
9. **Zhou, C., Cao, Z., Wei, G., Ke, W.** Research on Pyrolysis Characteristics of PE Outer Sheath of High-Voltage Cables Based on the Principle of Oxygen Consumption *Journal of Electrical Engineering & Technology* 18 2023: pp. 679–685. https://doi.org/10.1007/s42835-022-01178-0
10. **Zeng, W., Liu, T., Wang, Z., Tsukimoto, S., Saito, M., Ikuhara, Y.** Selective Detection of Formaldehyde Gas Using a Cd-doped TiO_2-SnO_2 Sensor *Sensors* 9 (11) 2019: pp. 9029–9038. https://doi.org/10.3390/s91109029
11. **Seo, M.H., Yuasa, M., Kida, T., Huh, J.S., Shimanoe, K., Yamazoe, N.** Gas Sensing Characteristics and Porosity Control of Nanostructured Films Composed of TiO_2 Nanotubes *Sensors and Actuators B: Chemical* 137 (2) 2009: pp. 513–520. https://doi.org/10.1016/j.snb.2009.01.057
12. **Nisar, J., Topalian, Z., De Sarkar, A., Österlund, L., Ahuja, R.** TiO_2-Based Gas Sensor: A Possible Application to SO_2 *ACS Applied Materials & Interfaces* 5 (17) 2013: pp. 8516–8522. https://doi.org/10.1021/am4018835
13. **Dachang, Ch., Ju, T., Xiaoxing, Z., Jiani, F., Yi, L., Ran, Z.** Detecting Decompositions of Sulfur Hexafluoride

Using Reduced Graphene Oxide Decorated with Pt Nanoparticles *Journal of Physics D: Applied Physics* 51 (18) 2018: pp. 185304. https://doi.org/10.1088/1361-6463/aaba95

14. **Mor, G.K., Varghese, O.K., Paulose, M., Shankar, K., Grimes, C.A.** A Review on Highly Ordered, Vertically Oriented TiO_2 Nanotube Arrays: Fabrication, Material Properties, and Solar Energy Applications *Solar Energy Materials and Solar Cells* 90 (14) 2006: pp. 2011 – 2075. https://doi.org/10.1016/j.solmat.2006.04.007
15. **Yao, W., Yingang, G., Chang, J., Zhou, Q., Li, J., Zhang, X.** Adsorption of SF_6 Decomposition Components on Pt3-TiO_2 (101) Surface: A DFT Study *Applied Surface Science* 459 (30) 2018: pp. 242 – 248. https://doi.org/10.1016/j.apsusc.2018.07.219
16. **Xiaoxing, Z., QinChuan, C., Weihua, H., Jinbin, Z.** Adsorptions of SO_2, SOF_2, and SO_2F_2 on Pt-Modified Anatase (101) Surface: Sensing Mechanism Study *Applied Surface Science* 353 2015: pp. 662 – 669. https://doi.org/10.1016/j.apsusc.2015.06.112
17. **Hao, S., Yingang, G., Huangli, W., Yingkai, L., Qian, W., Chao, T.** DFT Study of SF_6 Decomposed Products on Pd–TiO_2: Gas Sensing Mechanism Study *Adsorption* 25 (8) 2019: pp. 1643 – 1653. https://doi.org/10.1007/s10450-019-00150-1
18. **Xiaoxing, Z., Lei, Y., Jing, T., Dong, X.** Gas Sensitivity and Sensing Mechanism Studies on Au-Doped TiO_2 Nanotube Arrays for Detecting SF_6 Decomposed Components *Sensors* 14 (10) 2014: pp. 19517 – 19532. https://doi.org/10.3390/s141019517
19. **Delley, B.** From Molecules to Solids with the DMol^3 Approach *Journal of Chemical Physics* 113 2000: pp. 7756 – 7764. https://doi.org/10.1063/1.1316015
20. **Perdew, J.P., Burke, K., Ernzerhof, M.** Generalized Gradient Approximation Made Simple *Physical Review Letters* 77 (18) 1996: pp. 3865. https://doi.org/10.1103/PhysRevLett.77.3865
21. **Ju, W., Li, T., Su, X., Li, H., Li, X., Ma, D.** Au Cluster Adsorption on Perfect and Defective MoS_2 Monolayers: Structural and Electronic Properties *Physical Chemistry Chemical Physics* 19 (31) 2017: pp. 20735 – 20748. https://doi.org/10.1039/C7CP03062B
22. **Cao, Z., Li, W., Yao, Q., Zhang, H., Wei, G.** Platinum-Doped Anatase (101) Surface as Promising Gas-Sensor Materials for HF, CS_2, and COF_2: A Density Functional Theory Study *ACS Omega* 6 (1) 2020: pp. 696 – 701. https://doi.org/10.1021/acsomega.0c05235
23. **Tkatchenko, A., DiStasio, R.A.Jr., Head-Gordon, M., Scheffler, M.** Dispersion-Corrected Møller–Plesset Second-Order Perturbation Theory *The Journal of Chemical Physics* 131 (9) 2009: pp. 094106. https://doi.org/10.1063/1.3213194
24. **Yi, L., Xiaoxing, Z., Dachang, C., Song, X., Ju, T.** Adsorption Behavior of COF_2 and CF_4 Gas on the MoS_2 Monolayer Doped with Ni: A First-Principles Study *Applied Surface Science* 443 2018: pp. 74 – 279. https://doi.org/10.1016/j.apsusc.2018.02.252
25. **Cui, H., Liu, T., Zhang, Y., Zhang, X.X.** Ru-InN Monolayer as a Gas Scavenger to Guard the Operation Status of SF_6 Insulation Devices: A first-Principles Theory *IEEE Sensors Journal* 19 (13) 2019: pp. 5249 – 5255. https://doi.org/10.1109/JSEN.2019.2899966
26. **Song, X., Jun, Z., Xiaoxing, Z., Hao, C.** Pt-doped Single-Walled CNT as a Superior Media for Evaluating the Operation Status of Insulation Devices: A First-Principle Study *AIP Advances* 8 (10) 2018: pp. 105101. https://doi.org/10.1063/1.5050643
27. **Wanbayor, R., Ruangpornvisuti, V.** Adsorption of CO, H_2, N_2O, NH_3 and CH_4 on the Anatase TiO_2 (001) and (101) Surfaces and Their Competitive Adsorption Predicted by Periodic DFT Calculations *Materials Chemistry and Physics* 124 (1) 2010: pp. 720 – 725. https://doi.org/10.1016/j.matchemphys.2010.07.043
28. **Meiling, H., Xin, Z., Shandong, Y., Wanglai, C.** Double Graphitic-N Doping for Enhanced Catalytic Oxidation Activity of Carbocatalysts *Physical Chemistry Chemical Physics* 21 (10) 2019: pp. 5481 – 5488. https://doi.org/10.1039/C8CP07317A
29. **Zhengqin, C., Changli, Z., Jia, W., Gang, W., Ting, L., Kai, Z.** Theoretical Study of Adsorption Behavior of Dimethylamine and Ammonia on Al- and Ga-Doped BN Monolayer Surfaces Based on DFT *ACS Omega* 7 (42) 2022: pp. 37857 – 37866. https://doi.org/10.1021/acsomega.2c04963
30. **Yingang, G., Jinzhi, S., Pingan, Y., Tao, L., Chao, T., Lingna, X.** Platinum Modified MoS_2 Monolayer for Adsorption and Gas Sensing of SF_6 Decomposition Products: a DFT Study *High Voltage* 2020: pp. 41. https://doi.org/10.1049/hve.2019.0170
31. **Bechthold, P., Pronsato, M.E., Pistonesi, C.** DFT Study of CO Adsorption on Pd-SnO_2 (1 1 0) Surfaces *Applied Surface Science* 347 2015: pp. 291 – 298. https://doi.org/10.1016/j.apsusc.2015.03.149
32. **Hongbo, D.** The Adsorption of CO on Transition Metal Oxide Catalysts: a DFT Research. Wuhan Institute of Technology Wuhan, Hubei 430073, P. R. China, 2018. https://doi.org/10.27727/d.cnki.gwhxc.2019.000008
33. **Zhang, Y.H., Chen, Y.B., Zhou, K.G., Liu, C.H., Zeng, J., Zhang, H.L., Peng, Y.** Improving Gas Sensing Properties of Graphene by Introducing Dopants and Defects: A First-Principles Study *Nanotechnology* 20 (18) 2009: pp. 185504. https://doi.org/10.1088/0957-4484/20/18/185504
34. **Dachang, C., Xiaoxing, Z., Ju, T., Jiani, F., Yi, L., Huijun, L.** Adsorption and Dissociation Mechanism of SO_2 and H_2S on Pt Decorated Graphene: a DFT-D$_3$ Study *Applied Physics A* 124 (6) 2018: pp. 1 – 10. https://doi.org/10.1007/s00339-018-1827-7
35. **Dachang, C., Xiaoxing, Z., Ju, T., Hao, C., Yi, L.** Noble Metal (Pt or Au)-Doped Monolayer MoS_2 as a Promising Adsorbent and Gas-Sensing Material to SO_2, SOF_2 and SO_2F_2: a DFT Study *Applied Physics A* 124 (2) 2018: pp. 1 – 12. https://doi.org/10.1007/S00339-018-1629-Y
36. **Nosheen, U., Jalil, A., Ilyas, S.Z., Illahi, A., Khan, S.A., Hassan, A.** First-Principles Insight into a B4C3 Monolayer as a Promising Biosensor for Exhaled Breath Analysis *Journal of Electronic Materials* 51 (11) 2022: pp. 6568 – 6578. https://doi.org/10.1007/s11664-022-09898-9